Available online at www.sciencedirect.com
SCIENCE DIRECT®
International Journal of Mass Spectrometry 242 (2005) 5–11
International Journal of Mass Spectrometry
www.elsevier.com/locate/ijms

# Loss of benzene from methylphenylsilane and dimethylphenylsilane molecular cations

Joong Chul Choe*

*Department of Chemistry, University of Suwon, P.O. Box 77, Suwon 440-600, Korea*

Received 19 October 2004; accepted 16 November 2004
Available online 15 December 2004

**Abstract**

The dissociations of methylphenylsilane and dimethylphenylsilane molecular cations have been investigated by obtaining the 70-eV electron ionization mass spectra and the metastable ion decomposition spectra. Benzene loss from these molecular ions was noticeable compared to the dissociation of phenylsilane molecular cation. To understand the overall dissociation mechanisms, density functional theory calculations were performed at the B3LYP/6-311++G(d,p) level. It is proposed that the benzene loss occurs via the ion–molecule complexes formed by 1,2 shift of an α-H atom from the silicon to the *ipso*-carbon. The experimental observation that the dimethylphenylsilane ion loses benzene more easily than the methylphenylsilane ion can be understood by considering the stabilities of the product ions.


*Keywords:* Methylphenylsilane ion; Dimethylphenylsilane ion; Metastable ion; DFT calculation

## 1. Introduction

Mass spectrometry has been used to understand dissociation kinetics and mechanisms of gas phase molecular ions. Fragmentation pathways of molecular ions are determined efficiently using tandem mass spectrometry (MS/MS). Techniques such as metastable ion decomposition (MID), collision-induced dissociation, photodissociation, and neutralization–reionization have been widely employed for the purpose. Methods including isotopic labeling, peak shape analysis, and molecular orbital calculations provide valuable information for the elucidation of ionic dissociation mechanisms. Accuracy and confidence of theoretical estimations of energy data for dissociations are being better due to recent advances in calculation methods for electronic structures of molecular systems.

Mass spectrometric investigations on organosilicon molecules have provided us with opportunities to study different roles of the silicon and carbon atoms in unimolecular dissociations [1]. The dissociation of phenylsilane (**1a**) molecular cation is a good example [2–9]. As it is well known, the tropylium ion is produced from the toluene molecular cation as well as the benzylium ion [10–13]. It has been revealed, however, that the silatropylium ion is not produced from $\mathbf{1a}^{\bullet+}$, a silicon analogue of the toluene ion, through the studies by several researchers [5–9]. Such a difference could be understood by the theoretical expectation that the tropylium ion is more stable than the benzylium ion, while the reverse is true for their silicon analogues [9]. The other difference found is that the $H_2$ loss from $\mathbf{1a}^{\bullet+}$ is facile, while it is not from the toluene ion. This is presumably due to the difference lengths of the Si–H bonds as compared to the C–H bonds.

Detailed investigations on the dissociation mechanisms show some similarities as well as differences between the dissociations of the above-mentioned two molecular ions. The similar pathways have been proposed by quantum chemical calculations for the productions of the silatropylium ion [9] and its carbon analogue [11] from the respective molecular ions. Both of the pathways are initialized by 1,2 shift of an α-H atom from the silicon or carbon to the *ipso*-carbon. The isomer ($\mathbf{2a}^{\bullet+}$) thus formed from $\mathbf{1a}^{\bullet+}$, assigned as an

* Tel.: +82 31 220 2150; fax: +82 31 222 9385.
*E-mail address:* jcchoe@suwon.ac.kr.

1387-3806/$ – see front matter © 2004 Elsevier B.V. All rights reserved.
doi:10.1016/j.ijms.2004.11.010

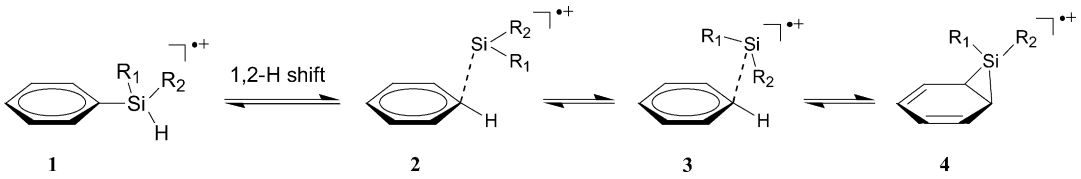


| Abbreviations | $R_1$ | $R_2$ |
|---|---|---|
| **1a** | H | H |
| **1b** | H | $CH_3$ |
| **1c** | $CH_3$ | $CH_3$ |

Scheme 1.

ion–molecule complex $C_6H_6{\cdot}SiH_2^{\bullet+}$, can form easily a bicyclic isomer ion (**4a**$^{\bullet+}$) via a conformer (**3a**$^{\bullet+}$). This isomerization pathway is shown in Scheme 1. The energies of these four isomers (**1a**$^{\bullet+}$–**4a**$^{\bullet+}$) are similar according to the previous molecular orbital calculation results [9]. The isomer **4a**$^{\bullet+}$ can form another isomer with a seven-membered ring and produce the silatropylium ion by H loss, but this process is energetically unfavorable compared to the other dissociation processes. By contrast, the carbon analogues of **2a**$^{\bullet+}$ and **4a**$^{\bullet+}$ are less stable than the toluene ion or the seven-membered-ring isomer, cycloheptatriene ion [14]. The production of tropylium ion through this route is energetically more favorable than that of benzylium ion. From such a difference, one can suggest that the ion–molecule complexes (**2a**$^{\bullet+}$ and **3a**$^{\bullet+}$) and the bicyclic isomer (**4a**$^{\bullet+}$), which interconvert with each other freely, may play a certain important role in the dissociation of phenylsilane ion unlike in that of toluene ion. The cleavage of the bond between the silicon and the *ipso*-carbon of the ion–molecule complexes is possible, which will produce the benzene radical cation and/or $SiH_2^{\bullet+}$. These fragment ions appear in the 70-eV electron ionization (EI) mass spectrum of phenylsilane reported previously [8]. Their relative abundances, however, were small and they were not detected in the MID of phenylsilane ion [9], suggesting that the Si–C bond cleavage needs high energies and are kinetically less favorable.

In this work, we examine the influence of methylation at the silicon atom of **1a**$^{\bullet+}$ on the dissociation mechanism and kinetics. The EI mass spectra of methylphenylsilane (**1b**), dimethylphenylsilane (**1c**), and trimethylphenylsilane have been obtained together with the MID spectra of their cations. Detailed investigations on the dissociations of these molecular cations have not been performed so far, while the dissociations of their carbon analogues, ethylbenzene [12,15–20], isopropylbenzene [15,16], and *tert*-butylbenzene [21–24] molecular cations have been studied extensively. The dissociation pathways and mechanisms of these ions will be discussed based on molecular orbital calculations with an emphasis on benzene loss.

## 2. Methods

### 2.1. Experimental

All experiments were performed using an Autospec orthogonal acceleration time-of-flight (oa-TOF) hybrid mass spectrometer (Micromass) of EBE-TOF geometry, located at the National Instrumentation Center for Environmental Management (NICEM) of Seoul National University. Samples were introduced into the ion source via a septum inlet and ionized by 70-eV EI. The ion source temperature was maintained at 200 °C, and ions generated were accelerated through 8 kV. For obtaining normal mass spectra, only the EBE analyzer was used and a photomultiplier was used as a detector. For MS/MS experiments, precursor ions accelerated to 8 keV were mass-selected by the EBE analyzer. The ions produced by MID in the forth field-free region were analyzed by the oa-TOF analyzer. Product ion spectra were obtained by pulsing deflector electrode placed after the collision cell assembly. A section of the ion beam containing the precursor and product ions, accelerated orthogonally by the pulse, entered the linear TOF analyzer. The ions were detected using a microchannel plate detector. All compounds were the best grade products from Aldrich and used without further purification.

### 2.2. Computational

Molecular orbital calculations were performed with the Gaussian 98 suite of programs [25] using an IBM SP Nighthawk-2 computer at the Computer Center of Seoul National University. Geometry optimizations for the several molecular ions, intermediates, and fragments were carried out at the unrestricted B3LYP (UB3LYP) density functional levels of theory using the 6-311++G(d,p) basis set. Transition state geometries connecting important stable structures were searched at the same level. All the TS geometries found were checked by calculating the intrinsic reaction coordinates at the 6-311++G(d,p) level for the dissociation of **1b**$^{\bullet+}$, and at the 6-31+G(d) level for that of **1c**$^{\bullet+}$. The harmonic vibrational frequencies and the zero-point energies for the optimized

structures were calculated at the UB3LYP/6-311++G(d,p) level, which were used without scaling. In all the reported energy data, the zero-point energies are included.

## 3. Results and discussion

### 3.1. Experimental observations

The mass spectrum of **1b** is shown in Fig. 1a. The main fragment ions are $C_7H_9Si^+$ (*m/z* 121), $C_7H_8Si^{\bullet+}$ (120), $C_6H_7Si^+$ (107), $C_6H_6Si^{\bullet+}$ (106), $C_6H_5Si^+$ (105), $C_2HSi^+$ (53), $CH_4Si^{\bullet+}$ (44), and $CH_3Si^+$ (43). To determine the dissociation pathways of $\mathbf{1b}^{\bullet+}$, the MID spectra of the molecular and fragment ions generated in the ion source were obtained. Since MID occurs not far above dissociation threshold in general, obtaining an MID spectrum is very useful in developing dissociation mechanisms especially when combined with the corresponding potential energy surfaces. The MID spectrum of the *m/z* 122 ion generated from **1b** is shown in Fig. 1b. Some product ions in the MID can originate from $^{12}C_6{}^{13}CH_9{}^{28}Si^+$, $^{12}C_7H_9{}^{29}Si^+$, and $^{12}C_7H_9{}^{30}Si^+$ as well as $^{12}C_7H_{10}{}^{28}Si^+$. Since the *m/z* 121 ions, mainly $^{12}C_7H_9{}^{28}Si^+$, are generated more abundantly than the *m/z* 122 ions by the EI (Fig. 1a), the contribution of its isotopic ions cannot be neglected in the MID of the *m/z* 122 ion. The main product ions in the MID of the *m/z* 121 ion were the *m/z* 43, 95, and 119 ions, with relative abundances of 100, 11, and 20, respectively. After the correction for the isotopic contribution, the main product ions in the MID of $^{12}C_7H_{10}{}^{28}Si^+$ are the *m/z* 121, 120, and 107 ions, of which relative abundances are similar to those shown in Fig. 1b. That is, most of the *m/z* 44 ions produced by the MID of the *m/z* 122 are $^{12}CH_3{}^{29}Si^+$ and $^{13}CH_3{}^{28}Si^+$, and most of the *m/z* 43 ions are $^{12}CH_3{}^{28}Si^+$. These originate from $^{12}C_6{}^{13}CH_9{}^{28}Si^+$ or $^{12}C_7H_9{}^{29}Si^+$ not from $^{12}C_7H_{10}{}^{28}Si^+$.

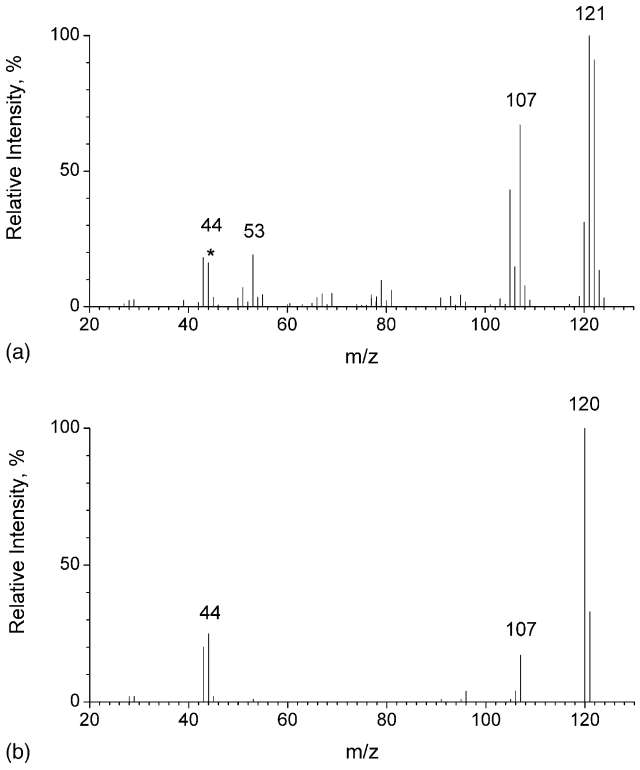


Fig. 1. (a) 70-eV EI mass spectrum of methylphenylsilane and (b) MS/MS product ion spectrum for the MID of the *m/z* 122 ion generated by EI of methylphenylsilane. Most of the *m/z* 44 and 43 ions produced in the MID originate from the isotopic ions of $^{12}C_7H_9{}^{28}Si^+$. See text for details. An asterisk identifies the peak by loss of benzene.

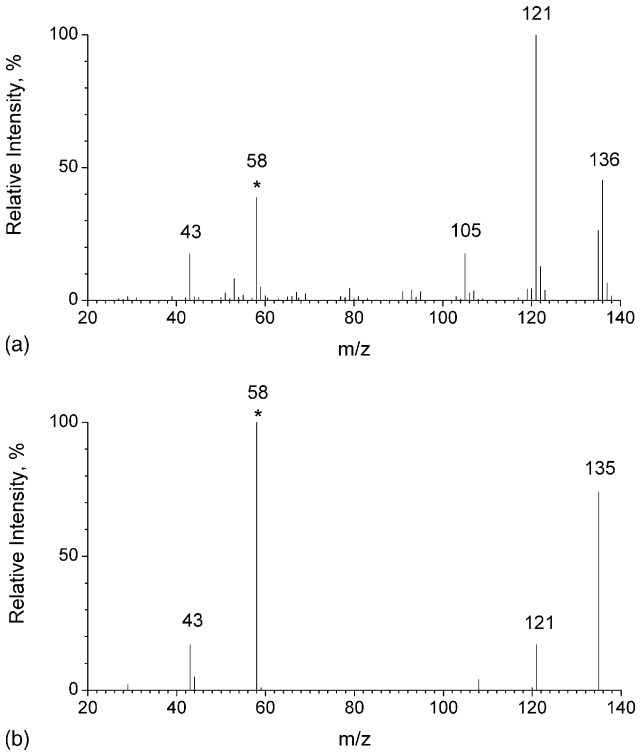


Fig. 2. (a) 70-eV EI mass spectrum of dimethylphenylsilane and (b) MS/MS product ion spectrum for the MID of the *m/z* 136 ion generated by EI of dimethylphenylsilane. About 40% of the *m/z* 43 ions produced in the MID originate from the isotopic ions of $^{12}C_8H_{11}{}^{28}Si^+$. See text for details. An asterisk identifies the peak by loss of benzene.

Apparently, the *m/z* 121 and 107 ions are produced by losses of H and $CH_3$, respectively, and the *m/z* 120 ion is produced by loss of $H_2$ via rearrangement. Detailed energetics on these dissociations will be described below. The other ions detected abundantly in the mass spectrum, but not in the MID, are formed mainly by consecutive dissociations. These were identified from the MID spectra of the fragment ions. The *m/z* 106 and 105 ions are produced mainly via the *m/z* 107 ion. The *m/z* 53 ion ($C_2HSi^+$), which has been observed also in the dissociation of $\mathbf{1a}^{\bullet+}$ and assigned as $HC{\equiv}C{-}Si^+$ in the previous work [8], is produced mainly by ring cleavages via the *m/z* 106 and 105 ions. The *m/z* 44 ion is produced by loss of $C_6H_6$, of which mechanism will be discussed below. The *m/z* 43 ion can be produced from the consecutive H and $C_6H_6$ losses and/or from the molecular ion via rearrangement.

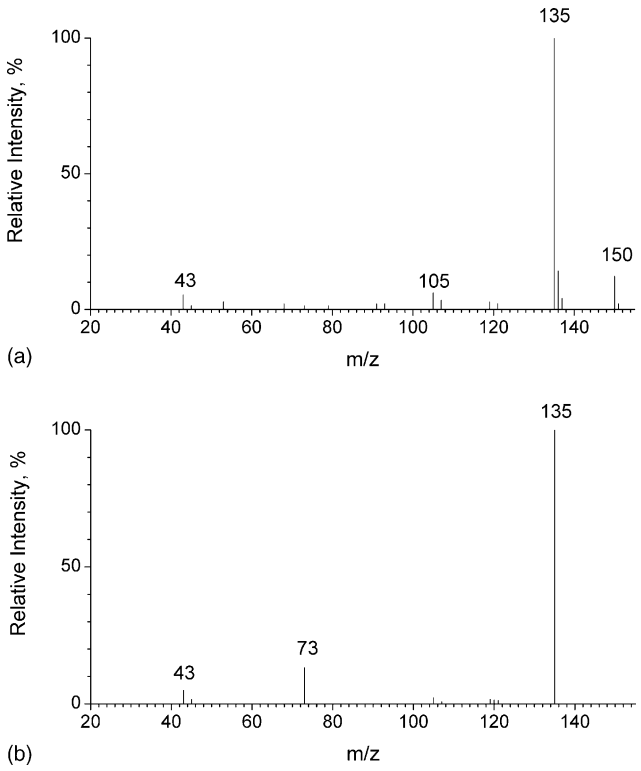


Fig. 3. (a) 70-eV EI mass spectrum of trimethylphenylsilane and (b) MS/MS product ion spectrum for the MID of the *m*/*z* 158 ion generated by EI of trimethylphenylsilane.

Fig. 2a shows the EI mass spectrum of **1c**. The main fragment ions are $C_8H_{11}Si^+$ (*m*/*z* 135), $C_7H_9Si^+$ (121), $C_6H_4Si^+$ (105), $C_2H_6Si^{\bullet+}$ (58), and $CH_3Si^+$ (43). To determine the dissociation pathways of $\mathbf{1c}^{\bullet+}$, the MID spectra of the molecular and fragment ions generated in the ion source were obtained. The MID spectrum of the *m*/*z* 136 ion generated from **1c** is shown in Fig. 2b. The contribution of the isotopic ions of $[M-1]^+$ was not large compared to the MID of $\mathbf{1b}^{\bullet+}$. The correction for the contribution reduced the relative abundance of the *m*/*z* 43 ion from 17 to about 10, but did not affect those of the *m*/*z* 135, 121, and 58 ions. Apparently, the *m*/*z* 135 and 121 ions are produced by losses of H and $CH_3$, respectively, and the *m*/*z* 58 ion is produced by loss of $C_6H_6$. The other abundant ions are produced mainly by consecutive dissociations, identified from the MID spectra of the fragment ions. The *m*/*z* 105 ion is produced mainly via the *m*/*z* 121 ion. The *m*/*z* 43 ion can be produced from the molecular, *m*/*z* 135 and 105 ions.

In the mass spectrum of trimethylphenylsilane (Fig. 3a), the *m*/*z* 135 ion formed by $CH_3$ loss is dominant. Also dominant was the $CH_3$ loss in the MID of the molecular ion (Fig. 3b). Loss of $C_6H_6$ does not occur from the molecular ion.

The dissociation patterns of the investigated molecular ions are similar to that of $\mathbf{1a}^{\bullet+}$ [8,9] in that the direct cleavages of the Si–R (R=H or $CH_3$) bonds and the loss of $H_2$ attached on the silicon atom are the main dissociation channels. Of course, the $H_2$ loss occurs only from $\mathbf{1a}^{\bullet+}$ and $\mathbf{1b}^{\bullet+}$. The most distinct difference in dissociation on methylation at the silicon atom is the enhancement of loss of $C_6H_6$, which will be identified as benzene below. In the mass spectrum of **1a**, the peak by $C_6H_6$ loss was very small [8], and it did not appear in the MID spectrum of $\mathbf{1a}^{\bullet+}$ [9]. The $C_6H_6$ loss is, however, important in the dissociations of $\mathbf{1b}^{\bullet+}$ and $\mathbf{1c}^{\bullet+}$ as described above, more significantly in the latter. This indicates that the $C_6H_6$ loss from $\mathbf{1b}^{\bullet+}$ and $\mathbf{1c}^{\bullet+}$ can compete effectively with the other main dissociation channels, while that from $\mathbf{1a}^{\bullet+}$ cannot. The fact that the $C_6H_6$ loss was not observed in the dissociation of trimethylphenylsilane ion, which does not have an α-H atom, suggests strongly that the ion–molecule complexes formed by the 1,2 shift of the α-H atom (Scheme 1) would be intermediates for the $C_6H_6$ loss from $\mathbf{1b}^{\bullet+}$ and $\mathbf{1c}^{\bullet+}$. Density functional theory (DFT) calculations were carried out to obtain the potential energy surfaces for the dissociations of $\mathbf{1b}^{\bullet+}$ and $\mathbf{1c}^{\bullet+}$, which will be used to understand the dissociation mechanisms and to gain insights into the $C_6H_6$ loss.

### 3.2. DFT calculations

The potential energy diagram constructed from the UB3LYP/6-311++G(d,p) calculations for the main dissociation pathways of $\mathbf{1b}^{\bullet+}$ is shown in Fig. 4. Similar to the dissociation of $\mathbf{1a}^{\bullet+}$ [9], the $H_2$ loss was the lowest-energy channel in the dissociation of $\mathbf{1b}^{\bullet+}$. It occurs by 1,1-elimination via a transition state lying 112.4 kJ mol$^{-1}$ above $\mathbf{1b}^{\bullet+}$. The H and $CH_3$ losses, which need somewhat larger energies than the $H_2$ loss, can occur directly from $\mathbf{1b}^{\bullet+}$. The product ions formed by these three processes correspond to the main peaks, the *m*/*z* 120, 121, and 105 ions, respectively, in the MID spectrum (Fig. 1b). Below the lowest dissociation limit, $\mathbf{1b}^{\bullet+}$ can undergo a rearrangement by 1,2 shift of an α-H atom from the silicon to the *ipso*-carbon to form an ion–molecule complex $\mathbf{2b}^{\bullet+}$, which freely interconverts with $\mathbf{3b}^{\bullet+}$ and $\mathbf{4b}^{\bullet+}$. $\mathbf{4b}^{\bullet+}$ can rearrange to the seven-membered-ring isomer $\mathbf{5b}^{\bullet+}$. The H and $CH_3$ losses from $\mathbf{5b}^{\bullet+}$, however, need larger energies than those occurring directly from $\mathbf{1b}^{\bullet+}$, respectively, and hence, are less important.

The mechanistic picture of the dissociations and isomerizations described so far is similar to that of $\mathbf{1a}^{\bullet+}$ [9] in that the production of silabenzylium ions is energetically more favorable than that of silatropylium ions. A noticeable difference can be found from the detection of the *m*/*z* 44 ion ($SiHCH_3^{\bullet+}$) with considerable abundance in the mass spectrum of **1b**, believed to be produced via ion–molecule complexes, while such an ion was detected negligibly in the mass spectrum of **1a**. The ion–molecule complexes, $\mathbf{2b}^{\bullet+}$ and $\mathbf{3b}^{\bullet+}$, can produce benzene and/or benzene radical cation by cleavage of the weak bond between the silicon and the *ipso*-carbon. The calculated Si–C bond lengths of $\mathbf{2b}^{\bullet+}$ and $\mathbf{3b}^{\bullet+}$ are 2.166 and 2.120 Å, respectively, longer than that of $\mathbf{1b}^{\bullet+}$ of 1.912 Å. The critical energies for these bond cleavages, with respect

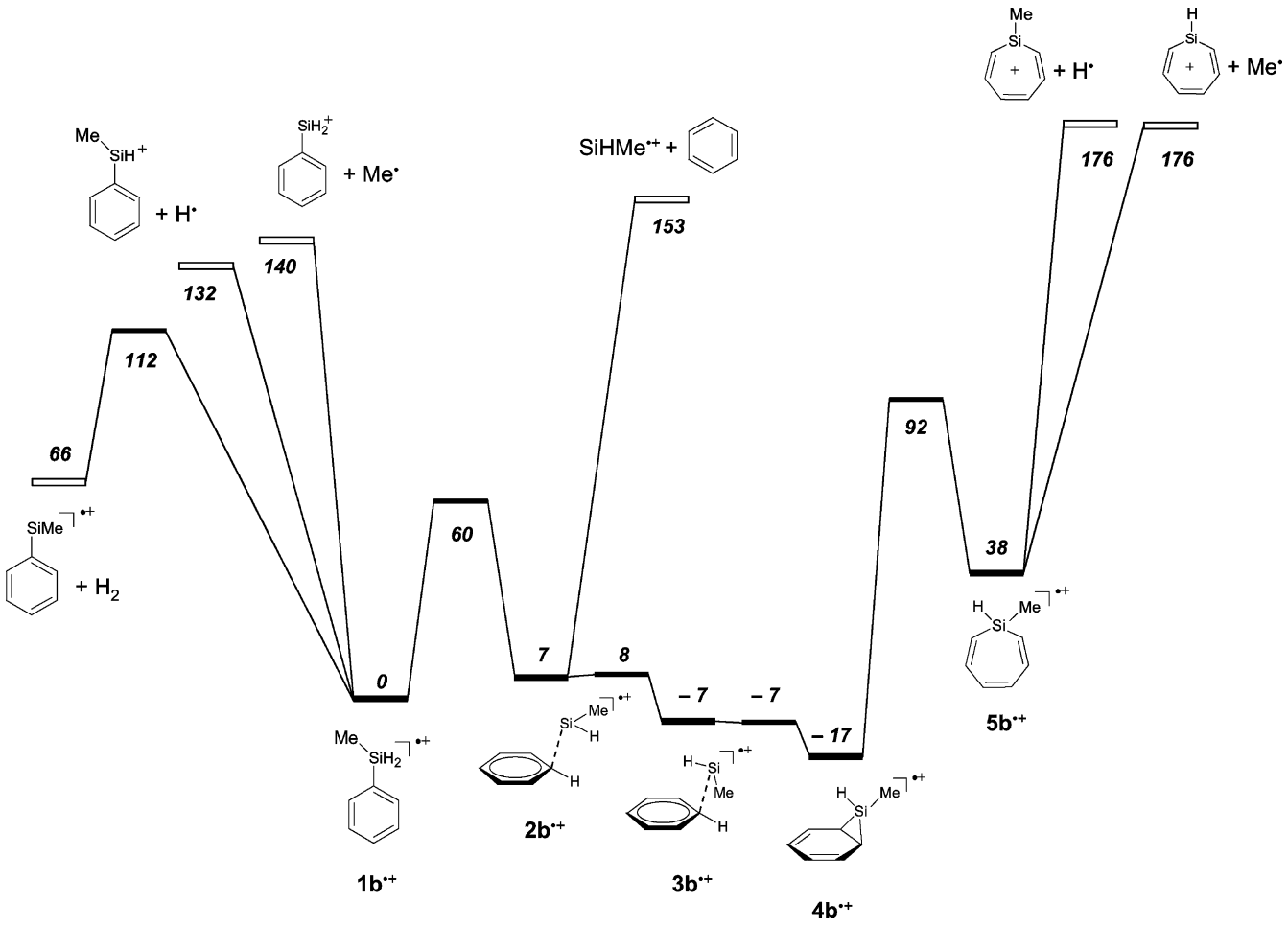


Fig. 4. Potential energy diagram for the isomerization and dissociation of methylphenylsilane ion derived from the UB3LYP/6-311++G(d,p) calculations. The italic numbers are the relative energies (in kJ mol$^{-1}$).

to **1b**$^{\bullet+}$, estimated from the DFT calculations are listed in Table 1 together with those for the other main dissociation channels. The loss of benzene, corresponding to the production of the *m*/*z* 44 ion, is energetically more favorable than the production of benzene ion, but its critical energy is somewhat higher than those of the H, $H_2$, and $CH_3$ losses. This means that it can compete with the main dissociation channels, agreeing with the observation of the peak at *m*/*z* 44 in the mass spectrum. By contrast, the loss of benzene from **1a**$^{\bullet+}$ needs far larger energy than those of other channels such as the H and $H_2$ losses (Table 1), indicating that it cannot compete effectively with the others.

Table 1
Critical energies[a] (in kJ mol$^{-1}$) for the formations of some product ions from phenylsilane ions calculated at the UB3LYP/6-311++G(d,p) DFT level

| Product ions | Molecular ions | | |
|---|---|---|---|
| | Phenylsilane$^{\bullet+}$[c] | Methylphenylsilane$^{\bullet+}$ | Dimethylphenylsilane$^{\bullet+}$ |
| [*M*–H]$^{+}$[b] | 158.9 | 132.3 | 112.4 |
| [*M*–$H_2$]$^{\bullet+}$ | 128.2 | 112.4 | – |
| [*M*–$CH_3$]$^{+}$[b] | – | 140.3 | 112.3 |
| [*M*–$C_6H_6$]$^{\bullet+}$ | 211.1 | 152.8 | 107.4 |
| $C_6H_6^{\bullet+}$ | 213.4 | 226.0 | 234.7 |

[a] Values with respect to the molecular ions.
[b] Silabenzylium structures.
[c] Reference [9].

There exist several pathways to produce the *m*/*z* 43 ion from **1b**$^{\bullet+}$. According to the present DFT calculations, $SiCH_3^+$ is the most stable among the possible isomeric *m*/*z* 43 ions, of which energy is smaller than $HSiCH_2^+$ by 166 kJ mol$^{-1}$. The most energetically favorable channel is loss of $C_6H_7$ (cyclohexadienyl radical) from another ion–molecule complex $C_6H_7{\cdot}SiCH_3^{\bullet+}$ formed via **2b**$^{\bullet+}$. Its calculated endoergicity is 246.7 kJ mol$^{-1}$. The $SiCH_3^+$ ion can be produced also by consecutive dissociations such as loss of $H_2$ and phenyl radical, loss of H and benzene, and loss of benzene and H. All the endoergicities of these consecutive dissociations estimated are larger than 340 kJ mol$^{-1}$. This suggests that the *m*/*z* 43 peak in the EI spectrum is the $SiCH_3^+$ ion produced mainly from the molecular ion via the ion–molecule complex $C_6H_7{\cdot}SiCH_3^{\bullet+}$.

The potential energy diagram constructed from the DFT calculations for the dissociations of **1c**$^{\bullet+}$ is qualitatively

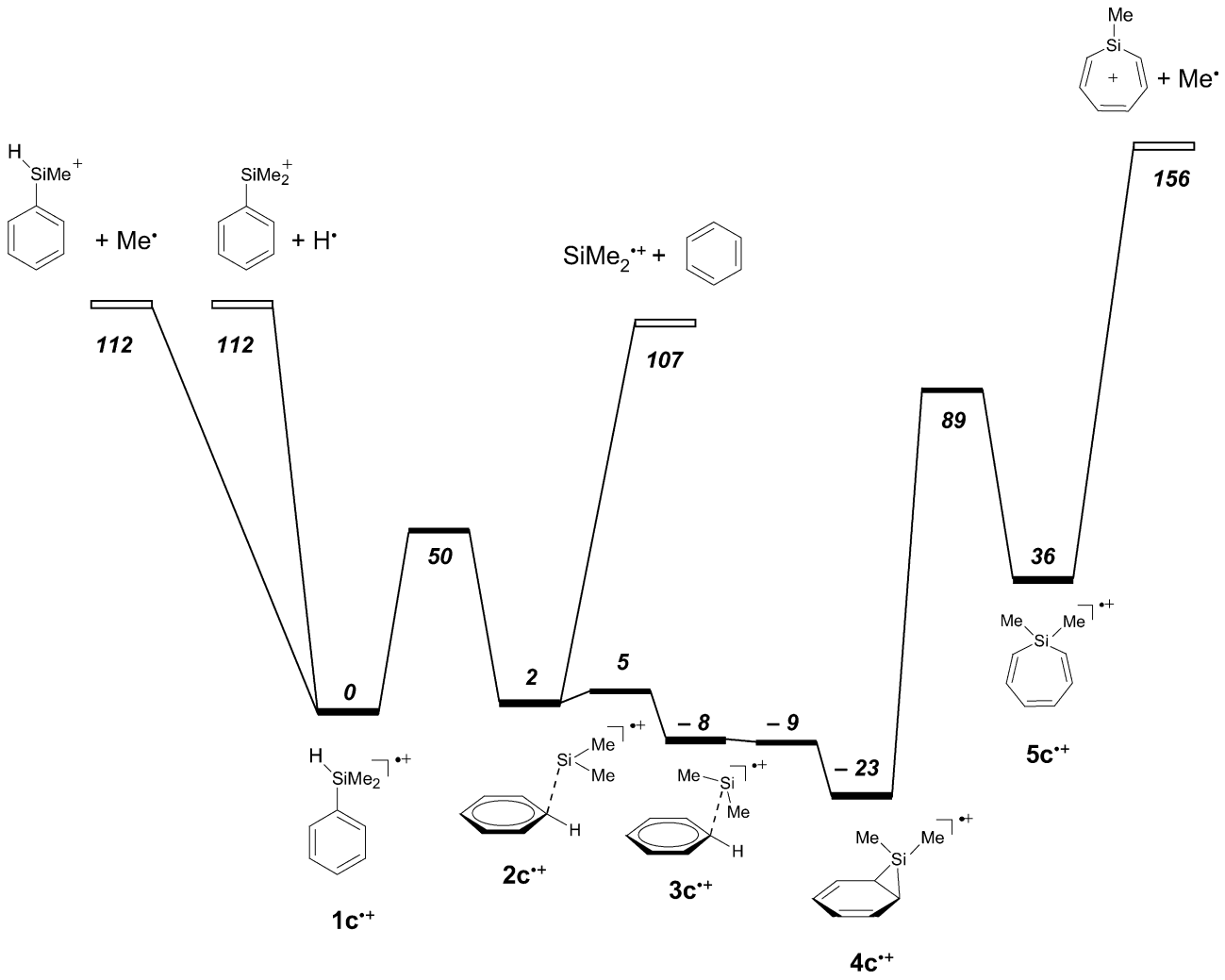


Fig. 5. Potential energy diagram for the isomerization and dissociation of dimethylphenylsilane ion derived from the UB3LYP/6-311++G(d,p) calculations. The italic numbers are the relative energies (in kJ mol$^{-1}$).

similar to that of **1b**$^{\bullet+}$ (Fig. 5). One difference is that the $H_2$ loss, occurring from **1b**$^{\bullet+}$, does not occur from **1c**$^{\bullet+}$ due to the presence of only one α-H atom. **1c**$^{\bullet+}$ can undergo easily a rearrangement by 1,2 shift of the α-H atom from the silicon to the *ipso*-carbon to form the stable isomers; **2c**$^{\bullet+}$, **3c**$^{\bullet+}$, and **4c**$^{\bullet+}$. The dissociation via the seven-membered-ring isomer is energetically unfavorable, similar to the cases of **1a**$^{\bullet+}$ and **1b**$^{\bullet+}$. The loss of benzene occurring via the ion–molecule complexes is estimated to be the lowest-energy dissociation channel (Table 1). This agrees well with the experimental observation of the intense peaks at *m*/*z* 58 in the EI and MID spectra (Fig. 2). The H and $CH_3$ losses are expected to occur from **1c**$^{\bullet+}$ easily also, agreeing with the experimental observations.

According to the estimated energy data (Table 1), benzene loss from the phenylsilane ion and its methyl derivatives becomes easier as the number of methyl substituents of the molecular ions increases. This tendency is mainly due to the different stabilities of the product ions formed by benzene loss. It is apparent that the extent of delocalization of the positive charge and hence, the stability increase in order of $SiH_2^{\bullet+}$, $SiHCH_3^{\bullet+}$, and $Si(CH_3)_2^{\bullet+}$. The data listed in Table 1 show that the critical energies for the H, $H_2$, and $CH_3$ losses also decrease as the number of methyl substituents of the molecular ions increases. This can be understood also by considering the stabilities of the product ions. The product ion with a methyl substituent is more stable relatively than that without, because of the more delocalized charge. Such a stabilization effect by methylation is larger in the benzene loss than in the other dissociation channels. Thus, the critical energy for the benzene loss becomes the smallest in the dissociation channels of **1c**$^{\bullet+}$, while it is larger than the H and $H_2$ losses in the dissociation of **1a**$^{\bullet+}$. The lack of benzene loss from the trimethylphenylsilane ion is reasonable because there is no α-H to migrate to the *ipso*-carbon and form an ion–molecule complex, a precursor necessary for benzene loss.

The most energetically favorable channel to produce the *m*/*z* 43 ion from $\mathbf{1c}^{\bullet+}$ is estimated to be loss of $C_6H_6CH_3$ (methylcyclohexadienyl radical) via $\mathbf{2c}^{\bullet+}$. Its calculated endoergicity is 296.4 kJ mol$^{-1}$. Among other possible consecutive dissociation channels, loss of $CH_3$ and benzene is the lowest-energy channel, of which endoergicity estimated is 320.2 kJ mol$^{-1}$. These are possible pathways for the production of the *m*/*z* 43 by the EI. The production of the *m*/*z* 43 ion in the MID, however, cannot be understood because the dissociations along these pathways need much higher energies compared to the H, $CH_3$, and $C_6H_6$ losses. It is possible that the *m*/*z* 43 ion is produced along another unusual pathway, more kinetically favorable than those mentioned above, which could not be identified in this work.

In contrast to $\mathbf{1b}^{\bullet+}$ and $\mathbf{1c}^{\bullet+}$, the ethylbenzene and isopropylbenzene ions do not undergo benzene loss [26]. It is known that the ethylbenzene ion undergoes the dissociation to methyltropylium ion after a 1,2 shift of an α-H atom to the *ipso*-carbon rather than benzene loss [19,20].

## 4. Conclusions

The general mechanistic picture of the isomerizations and dissociations of methylphenylsilane and dimethylphenylsilane ions deduced from the experimental and theoretical investigations is similar to that of phenylsilane ion. It has been found, however, that methylation at the silicon atom of the phenylsilane ion affects significantly the yield of benzene loss. As the number of methyl substituents increases, the benzene loss becomes more important. In the dissociation of trimethylphenylsilane ion, however, the benzene loss was not observed. The DFT calculations lead to the conclusion that the benzene loss from methylphenylsilane and dimethylphenylsilane ions occurs via the ion–molecule complexes formed by 1,2 shift of an α-H atom from the silicon to the *ipso*-carbon. The tendency of benzene loss can be understood by the relative stabilities of the product ions.

## Acknowledgements

This work was supported by the Korea Research Foundation Grant (KRF-2003-015-C00280). The author thanks Jiyoon Lee of NICEM for technical assistance.

## References

[1] H. Schwarz, in: S. Patai, Z. Rappoport (Eds.), The Gas Phase in the Chemistry of Organic Silicon Compounds, Wiley, Chichester, 1989 (Chapter 7).
[2] F. Bohlmann, C. Köppel, H. Schwarz, Org. Mass Spectrom. 9 (1974) 622.
[3] S. Murthy, Y. Nagano, J.L. Beauchamp, J. Am. Chem. Soc. 114 (1992) 3573.
[4] Y. Nagano, S. Murthy, J.L. Beauchamp, J. Am. Chem. Soc. 115 (1993) 10805.
[5] A. Nicolaides, L. Radom, J. Am. Chem. Soc. 116 (1994) 9769.
[6] A. Nicolaides, L. Radom, J. Am. Chem. Soc. 118 (1996) 10561.
[7] R.L. Jarek, S.K. Shin, J. Am. Chem. Soc. 119 (1997) 6376.
[8] J.C. Choe, Rapid Commun. Mass Spectrom. 17 (2003) 207.
[9] J.C. Choe, Int. J. Mass Spectrom. 237 (2004) 1.
[10] C. Lifshitz, Acc. Chem. Res. 27 (1994) 138 (and references therein).
[11] C. Lifshitz, Y. Gotkis, A. Ioffe, J. Laskin, S. Shaik, Int. J. Mass Spectrom. Ion Processes 125 (1993) R7.
[12] D. Kuck, Mass Spectrom. Rev. 9 (1990) 187.
[13] J.H. Moon, J.C. Choe, M.S. Kim, J. Phys. Chem. A 104 (2000) 458.
[14] From Ref. [11]. Since the calculations in the reference were carried out at low levels, this was confirmed by the UB3LYP/6-311++G(d,p) DFT calculations in this work.
[15] R.G. McLoughlin, J.D. Morrison, J.C. Traeger, Org. Mass Spectrom. 14 (1979) 104.
[16] B.J. Stapleton, R.D. Bowen, D.H. Williams, J. Chem. Soc., Perkin Trans. 2 (1979) 1219.
[17] J. Grotemeyer, H.-F. Grützmacher, Org. Mass Spectrom. 17 (1982) 353.
[18] P. Ausloos, J. Am. Chem. Soc. 104 (1982) 5259.
[19] T.D. Fridgen, J. Troe, A.A. Viggiano, A.J. Midey, S. Williams, T.B. McMahon, J. Phys. Chem. A 108 (2004) 5600.
[20] Y.H. Kim, J.C. Choe, M.S. Kim, J. Phys. Chem. A 105 (2001) 5751.
[21] E.S. Mukhatar, R.E. Griffiths, R.E. March, F.M. Harris, J.H. Beynon, Int. J. Mass Spectrom. Ion Phys. 41 (1981) 61.
[22] W.A. Brand, T. Baer, Int. J. Mass Spectrom. Ion Phys. 49 (1983) 103.
[23] W.A. Brand, K. Levsen, Int. J. Mass Spectrom. Ion Phys. 51 (1983) 135.
[24] Y.S. Cho, J.C. Choe, M.S. Kim, J. Phys. Chem. 99 (1995) 8645.
[25] M.J. Frisch, G.W. Trucks, H.B. Schlegel, G.E. Scuseria, M.A. Robb, J.R. Cheeseman, V.G. Zakrzewski, J.A. Montgomery, Jr., R.E. Stratmann, J.C. Burant, S. Dapprich, J.M. Millam, A.D. Daniels, K.N. Kudin, M.C. Strain, O. Farkas, J. Tomasi, V. Barone, M. Cossi, R. Cammi, B. Mennucci, C. Pomelli, C. Adamo, S. Clifford, J. Ochterski, G.A. Petersson, P.Y. Ayala, Q. Cui, K. Morokuma, N. Rega, P. Salvador, J.J. Dannenberg, D.K. Malick, A.D. Rabuck, K. Raghavachari, J.B. Foresman, J. Cioslowski, J.V. Ortiz, A.G. Baboul, B.B. Stefanov, G. Liu, A. Liashenko, P. Piskorz, I. Komaromi, R. Gomperts, R.L. Martin, D.J. Fox, T. Keith, M.A. Al-Laham, C.Y. Peng, A. Nanayakkara, M. Challacombe, P.M.W. Gill, B. Johnson, W. Chen, M.W. Wong, J.L. Andres, C. Gonzalez, M. Head-Gordon, E.S. Replogle, J.A. Pople, Gaussian 98 (Revision A.11.3), Gaussian Inc., Pittsburgh, PA, 2002.
[26] NIST Chemistry WebBook: NIST Standard Reference Database Number 69, March 2003.